Dear Author,

Here are the proofs of your article.

- You can submit your corrections **online**, via **e-mail** or by **fax**.
- For **online** submission please insert your corrections in the online correction form. Always indicate the line number to which the correction refers.
- You can also insert your corrections in the proof PDF and **email** the annotated PDF.
- For fax submission, please ensure that your corrections are clearly legible. Use a fine black pen and write the correction in the margin, not too close to the edge of the page.
- Remember to note the **journal title**, **article number**, and **your name** when sending your response via e-mail or fax.
- **Check** the metadata sheet to make sure that the header information, especially author names and the corresponding affiliations are correctly shown.
- **Check** the questions that may have arisen during copy editing and insert your answers/ corrections.
- **Check** that the text is complete and that all figures, tables and their legends are included. Also check the accuracy of special characters, equations, and electronic supplementary material if applicable. If necessary refer to the *Edited manuscript*.
- The publication of inaccurate data such as dosages and units can have serious consequences. Please take particular care that all such details are correct.
- Please **do not** make changes that involve only matters of style. We have generally introduced forms that follow the journal's style.
  Substantial changes in content, e.g., new results, corrected values, title and authorship are not allowed without the approval of the responsible editor. In such a case, please contact the Editorial Office and return his/her consent together with the proof.
- If we do not receive your corrections **within 48 hours**, we will send you a reminder.
- Your article will be published **Online First** approximately one week after receipt of your corrected proofs. This is the **official first publication** citable with the DOI. **Further changes are, therefore, not possible.**
- The **printed version** will follow in a forthcoming issue.

Please note

After online publication, subscribers (personal/institutional) to this journal will have access to the complete article via the DOI using the URL: http://dx.doi.org/[DOI].
If you would like to know when your article has been published online, take advantage of our free alert service. For registration and further information go to: http://www.link.springer.com.

Due to the electronic nature of the procedure, the manuscript and the original figures will only be returned to you on special request. When you return your corrections, please inform us if you would like to have these documents returned.

Metadata of the article that will be visualized in OnlineFirst

ArticleTitle	Predicting the risk of kidney stone formation in the nephron by ‘reverse engineering’	
Article Sub-Title		
Article CopyRight	Springer-Verlag GmbH Germany, part of Springer Nature (This will be the copyright line in the final PDF)	
Journal Name	Urolithiasis	
Corresponding Author	Family Name	**Königsberger**
	Particle	
	Given Name	**Erich**
	Suffix	
	Division	Chemistry
	Organization	Murdoch University
	Address	Murdoch, WA, 6150, Australia
	Phone	
	Fax	
	Email	e.koenigsberger@murdoch.edu.au
	URL	
	ORCID	http://orcid.org/0000-0002-4606-0741
Author	Family Name	**Hill**
	Particle	
	Given Name	**Michael G.**
	Suffix	
	Division	Chemistry
	Organization	Murdoch University
	Address	Murdoch, WA, 6150, Australia
	Phone	
	Fax	
	Email	m.hill@murdoch.edu.au
	URL	
	ORCID	
Author	Family Name	**May**
	Particle	
	Given Name	**Peter M.**
	Suffix	
	Division	Chemistry
	Organization	Murdoch University
	Address	Murdoch, WA, 6150, Australia
	Phone	
	Fax	
	Email	p.may@murdoch.edu.au
	URL	

ORCID

Schedule	Received	17 July 2019
	Revised	
	Accepted	12 November 2019

Abstract	Although most kidney stones are found in the calyx, they are usually initiated upstream in the nephron by precipitation there of certain incipient mineral phases. The risk of kidney stone formation can thus be indicated by changes in the degree of saturation of these minerals in the nephron fluid. To this end, relevant concentration profiles in the fluid along the nephron have been calculated by starting with specified urine compositions and imposing constraints from the corresponding, much less variable, blood compositions. A model for supersaturation within ten sections of both long and short nephrons has accordingly been developed based on this 'reverse engineering' of the necessary substance concentrations coupled with chemical speciation distributions calculated by our joint expert speciation system. This allows the likelihood of precipitation to be assessed based on Ostwald's 'Rule of Stages'. Differences between normal and stone-former profiles have been used to identify sections in the nephron where conditions seem most likely to induce heterogeneous nucleation.

Keywords (separated by '-')	Urinalysis - Brushite - Computer modelling - Ostwald's 'Rule of Stages' - Joint expert speciation system
Footnote Information	

Urolithiasis
https://doi.org/10.1007/s00240-019-01172-8

ORIGINAL PAPER

Predicting the risk of kidney stone formation in the nephron by 'reverse engineering'

Michael G. Hill[1] · Erich Königsberger[1] · Peter M. May[1]

Received: 17 July 2019 / Accepted: 12 November 2019

Abstract

Although most kidney stones are found in the calyx, they are usually initiated upstream in the nephron by precipitation there of certain incipient mineral phases. The risk of kidney stone formation can thus be indicated by changes in the degree of saturation of these minerals in the nephron fluid. To this end, relevant concentration profiles in the fluid along the nephron have been calculated by starting with specified urine compositions and imposing constraints from the corresponding, much less variable, blood compositions. A model for supersaturation within ten sections of both long and short nephrons has accordingly been developed based on this 'reverse engineering' of the necessary substance concentrations coupled with chemical speciation distributions calculated by our joint expert speciation system. This allows the likelihood of precipitation to be assessed based on Ostwald's 'Rule of Stages'. Differences between normal and stone-former profiles have been used to identify sections in the nephron where conditions seem most likely to induce heterogeneous nucleation.

Keywords Urinalysis · Brushite · Computer modelling · Ostwald's 'Rule of Stages' · Joint expert speciation system

Introduction

Kidney stones are a widespread and increasingly common medical problem with serious personal consequences and high economic costs [1–3]. Preventative strategies are needed to minimise surgical interventions but, despite much research, have been hindered by poor understanding of the underlying fundamental science [4]. Factors leading to kidney stone initiation are a key issue but have proved particularly troublesome. While numerous approaches have been proposed based on the analyses of urine composition [5–7], these have all so far overlooked the changing concentration profiles which prevail upstream and actually determine the conditions under which any solid phase must first be precipitated. This deficiency has now been addressed by straightforward calculations of fluid composition in the nephron using available literature information on how blood plasma filtrate is progressively concentrated to yield a given urine analysis [8]. Estimates for the logarithm of the Saturation Index, log(SI), with selected target minerals then allow their propensity to precipitate over the length of the nephron to be assessed and correlated with existing data from two different types of known kidney stone formers. Further insights improving the predictability of stone formation, especially recurrence, can be expected as more clinical correlations become available.

While the mechanisms of development of uric acid, infection and cystine stones are understood and methods to treat them successfully are available [3], the majority of calcium oxalate stones are idiopathic. The location of clinically significant stones is normally in the calyx, but it is apparent that the formation of calcium-based stones has its origin in the nephron [9–14]. Since urinary supersaturation with calcium oxalate monohydrate (COM) is apparently never high enough to result in homogeneous nucleation, heterogeneous nucleation must be taking place on some nucleating substrate [15, 16]. Hydroxyapatite, brushite, and uric acid may all serve as substrates for calcium oxalate monohydrate precipitation [11–13, 15–17].

Recent work has suggested that calcium oxalate stone formation is based on calcium phosphate precipitation higher

✉ Erich Königsberger
e.koenigsberger@murdoch.edu.au

Michael G. Hill
m.hill@murdoch.edu.au

Peter M. May
p.may@murdoch.edu.au

[1] Chemistry, Murdoch University, Murdoch, WA 6150, Australia

up in the nephron. In particular, the "*Calcium Phosphate Hypothesis*" proposes a mechanism where calcium oxalate stones are formed as the result of an initial precipitation of calcium phosphate [18]. This is supported by findings that calcium phosphate activity products have been found to be significantly higher in the urine of calcium oxalate stone formers [19]. The complex interactions of the ions present in nephron fluid highlights the importance of understanding the mechanisms underlying the processes [18, 20] and the contribution that can be made by chemical speciation models.

Most calcium oxalate stones contain a small proportion of calcium phosphate, often in the core of the stone, indicating that calcium phosphate is a common initial crystal phase [3, 12]. High levels of supersaturation of calcium phosphate and higher pH can be found in the loop of Henle and the distal tubule, resulting in the precipitation of calcium phosphate [9, 14, 18]. Further along in the nephron, if the pH is sufficiently low in the collecting duct, these calcium phosphate crystals will dissolve, bringing about sufficient levels of calcium and oxalate concentration for crystal nucleation or additional growth of an existing calcium oxalate stone to occur [11, 12, 14]. It is reasonable to think that in the case where all of the calcium phosphate crystals dissolve, the resultant stone will be a calcium oxalate stone but where some of the calcium phosphate remains undissolved, a mixed stone may result. Whether, and how, the initial calcium phosphate precipitation can be counteracted is not yet known but is now an active focus of research [3]. However, it has been suggested that avoiding low pH in these late nephron sections can prevent the dissolution of calcium phosphate [3]. The administration of alkali augments urinary macromolecule inhibitory power as well as increasing urinary citrate [3].

It is known that hydroxyapatite is supersaturated throughout the length of the nephron [9] and that there is a risk of calcium phosphate precipitation both in the ascending limb of the loop of Henle and the distal tubule [3]. Locations where nucleation is most likely to occur are the end of the descending loop of Henle and the end of the collecting ducts [21]. However, it is not known which phase of calcium phosphate is the first to precipitate [22]. It seems likely that the precipitation preceding the formation of hydroxyapatite (HAP) would be of amorphous calcium phosphate (ACP), $Ca_xH_y(PO_4)_z \cdot nH_2O$, octacalcium phosphate (OCP), $Ca_8H_2(PO_4)_6 \cdot 5H_2O$, or brushite (BRU), $CaHPO_4 \cdot 2H_2O$ [13, 22–25]. Identification of this initially formed phase would obviously be important. While magnesium ions have been shown to inhibit the crystallisation and growth of HAP and OCP, the same effect is not seen in the case of BRU [26]. Pak et al. [27–31] consider BRU to be the phase that initially precipitates, based on observations that this phase has the highest nucleation rate amongst the calcium phosphates.

Ostwald's Rule of Stages states that the formation of the least stable phases precedes the thermodynamically stable phase [4, 22, 32]. In accord with this prediction, the first solid to precipitate will be the one that is least supersaturated [9]. The results in Table 1, where the blood plasma value for calcium has been increased to simulate stone-forming pathology, indicate that BRU is the supersaturated substance with the lowest SI value under the conditions in the ascending loop of Henle and thus, BRU seems to be the substance most likely to precipitate [4]. This is in agreement with a number of studies [9, 25, 27]. Thus, for the purposes of analysis of the results of the calculations that follow, it has been assumed that BRU is the calcium phosphate phase that will be the first one to precipitate; hence, the risk of calcium phosphate precipitation has been based on the log(SI) values for BRU.

Table 1 log(SI) values for stone-forming salts under a simulated increased calcium load

Nephron section[a]	Salt			
	$CaC_2O_4 \cdot H_2O$ (COM)	$CaHPO_4 \cdot 2H_2O$ (BRU)	$Ca_4H(PO_4)_3 \cdot 2.5H_2O$ (OCP)	$Ca_5(OH)(PO_4)_3$ (HAP)
BC	− 0.9825	− 0.1161	3.8860	10.3500
PT	− 0.7199	− 0.3117	2.0830	7.3300
PR	− 0.3336	− 0.4629	1.4400	6.4980
tDL	− 0.01538	0.02508	4.7070	11.4300
tAL	− 0.01451	0.02127	4.4980	11.0200
MD	− 0.01280	− 0.0639	3.3080	9.0380
DT	− 0.05509	− 0.1333	2.9610	8.5510
CT	− 0.2177	− 0.5262	0.3986	4.6050
CCD	0.1378	− 0.3533	0.5469	4.4770
MCD	0.2990	− 0.4214	− 0.2115	3.1650
CX	0.8032	0.3771	2.7170	6.3630

[a]See Fig. 1

Journal : Large 240 | Article No : 1172 | Pages : 8 | MS Code : 1172 | Dispatch : 18-11-2019

Experimental evidence supporting this assumption has been provided by recent in vitro studies using atomic force microscopy [33]. These have shown it is likely that BRU is significant in early phases of stone formation, but transforms to HAP via ACP and OCP through dissolution and reprecipitation under the physiologic conditions (including varying supersaturation) found in the kidney. Thus, BRU will be a less common phase found in kidney stones, as much of it will have transformed into HAP by the time the stones become clinically significant.

Methods

During the process of converting glomerular filtrate into urine, the fluid passing through the nephron undergoes significant concentration changes for dissolved substances [34]. A computer model has recently been developed to simulate these concentration changes in the fluid within the kidney as it passes through the nephron [4, 8]. Based on published values of how the concentration of the various substances in the nephron vary during the transformation from blood plasma to urine [9, 11, 12, 14, 23, 24, 35], concentrations for a set of substances are calculated at a number of points in the nephron, for both long and short nephrons. Total concentrations of sodium, potassium, calcium, magnesium, chloride, phosphate, oxalate, sulfate, citrate, creatinine, urea, urate, ammonia, bicarbonate and pH are included in the data set. The path through the nephron is divided into sections, numbered from 0 to 10, as shown in Fig. 1. For each section, secretion and reabsorption coefficients were evaluated from published values [4]. Further details about the calculation procedure and availability of the computer program are given in "Appendix".

The present simulation produces a set of concentration values for each section in the nephron by 'reverse engineering'. Starting from measured urine compositions and being constrained by the corresponding blood compositions, the reabsorption coefficients of our original model [4] are proportionally adjusted to arrive at the concentrations in the fluid within each section of the nephron.

These values are then used as input to the joint expert speciation system (JESS) [36–39] to calculate log(SI) values, which are a measure of supersaturation, for calcium oxalate hydrates and various calcium phosphates. JESS is routinely made available to third-party academic users under licence. Details can be found on the website http://jess.murdoch.edu.au, including information about the 'Urine Expert' module which provides a convenient up-to-date interface for calculating mineral SI values for urine solutions of given composition.

Given the concentrations of a set of substances in blood plasma and urine, the model presented here can be used to calculate how properties of the fluid vary over the length of the nephron in terms of stone formation risk. In determining the precipitation risk for calcium phosphate, the log(SI) value for BRU is used, as noted above.

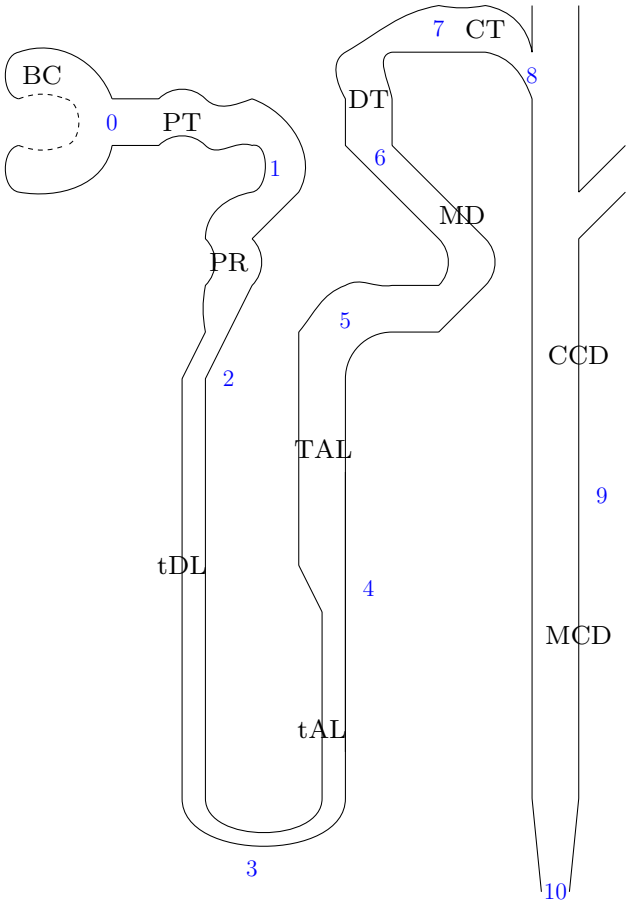

Fig. 1 Nephron coordinates used in calculations. *BC* Bowman's capsule, *PT* proximal tubule, *PR* pars recta, *tDL* thin descending limb, *tAL* thin ascending limb, *TAL* thick ascending limb, *MD* macula densa, *DT* distal tubule, *CT* connecting tubule, *CCD* cortical collecting duct, *MCD* medullary collecting duct

Data sets have been constructed accordingly using blood plasma and urine values from Robertson [10], as shown in Table 2, for a set of average values from normal subjects and sets from two different types of stone formers. The normal subjects are labelled UK N in the figures, and the two sets of recurrent stone formers are one set from the United Kingdom, labelled UK RSF, and one from the Kingdom of Saudi Arabia, labelled KSA RSF.

Results and discussion

The differences in log(SI) values along the path of a long nephron for BRU and COM are shown in Figs. 2 and 3. The stone type for the patients from Saudi Arabia is calcium

Journal : Large 240 | Article No : 1172 | Pages : 8 | MS Code : 1172 | Dispatch : 18-11-2019

Table 2 Blood and urine data of controls and stone formers [10]

Substance	UK N	UK RSF	KSA RSF
Blood			
Ultrafiltrable calcium, mmol/L	1.47	1.50	1.47
Ultrafiltrable phosphate, mmol/L	1.00	1.60	1.60
Oxalate, µmol/L	1.50	1.65	1.79
pH	7.38	7.38	7.38
Sodium, mmol/L	140	144	140
Potassium, mmol/L	4.0	4.2	4.0
Ultrafiltrable magnesium, mmol/L	0.60	0.56	0.56
Citrate, µmol/L	100	66	35
Sulfate, µmol/L	400	500	550
Urate, µmol/L	280	380	490
Ammonium, µmol/L	100	100	100
Urine			
Volume, L	1.72	1.43	1.34
pH	5.97	6.15	5.38
Calcium, mmol/day	5.62	9.05	5.09
Phosphate, mmol/day	28.9	47.8	49.6
Oxalate, mmol/day	0.34	0.55	0.82
Magnesium, mmol/day	3.93	3.64	3.67
Sodium, mmol/day	156	159	156
Potassium, mmol/day	71	74	71
Ammonium, mmol/day	22	18	45
Citrate, mmol/day	2.89	1.90	1.01
Sulfate, mmol/day	20	25	27
Uric acid, mmol/day	3.02	4.09	5.27

oxalate [10]. It can be seen in Fig. 2 that BRU is well below supersaturation for most of the collecting duct, which fits the characteristics of this case. There is a sharp drop in the value in the early part of the collecting duct. The UK RSF group contains both calcium oxalate and calcium phosphate stone formers [10]; hence, the higher log(SI) values for BRU shown in the plot is as expected. In the case of COM, the value is higher for both sets of stone formers than that for the normal set, all along the nephron, with the values for the recurrent stone formers from the Kingdom of Saudi Arabia being higher than the United Kingdom set, especially in the middle parts of the nephron. In both sets of stone formers, the increase in the log(SI) value of BRU in the mid-nephron, followed by the sharp decrease in value in the collecting duct, where COM supersaturation is rising well above normal supersaturation values illustrated here is a scenario where any BRU that may have precipitated further up the nephron may (partially) dissolve in the collecting duct, enhancing the crystallisation of COM. Consequently, this process is a combination of (1) the presence of the BRU crystals to act as a heterogeneous nucleant and (2) the increase in calcium ion concentration resulting from the incomplete dissolution of BRU crystals, in accordance with the "*Calcium Phosphate Hypothesis*" [18].

Figure 2 shows log(SI) of BRU and Figure 5 in [10] shows log(RSS) of OCP for UK N, UK RSF and KSA RSF, where RSS denotes relative supersaturation. A similar general pattern can be seen, with the two stone-forming sets having a higher saturation in the middle sections of the nephron, the KSA RSF subjects falling below the other two towards the

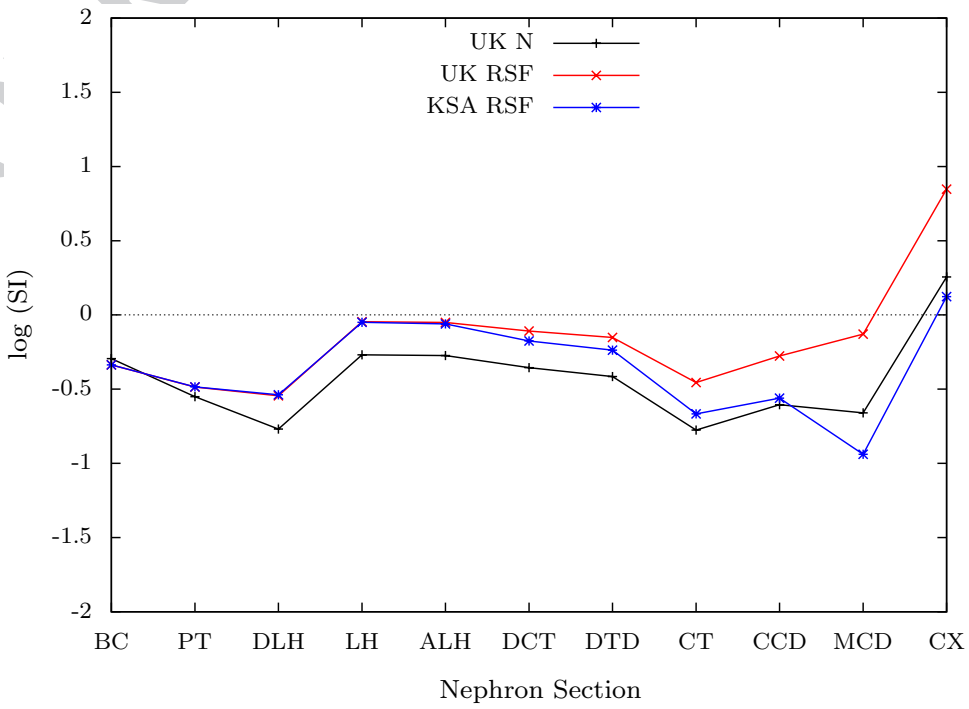

Fig. 2 Supersaturation of BRU: normal and stone former profiles. Sections of long nephron—the points on the *x*-axis correspond to the coordinates 0–10 in Fig. 1

Journal : Large 240 | Article No : 1172 | Pages : 8 | MS Code : 1172 | Dispatch : 18-11-2019

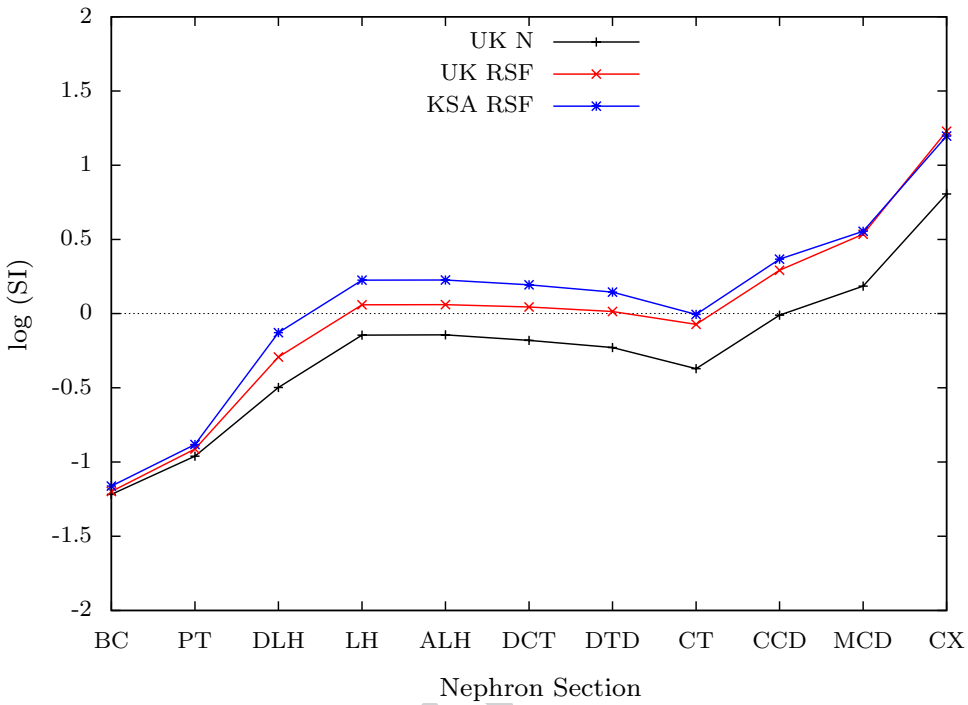

Fig. 3 Supersaturation of COM: normal and stone-former profiles. Sections of long nephron as in Fig. 2

end of the nephron and the UK RSF subject saturation level rising above the others toward the end of the nephron.

Figure 2 in [10] shows log(RSS) of CaOx along the nephron for UK N, UK RSF and KSA RSF. Comparing this to Fig. 3, the changes in saturation between the three groups follow the same pattern. Supersaturation is attained in the loop of Henle for both sets of stone formers, but not in the case of the controls. Supersaturation increases toward the end the nephron in all three cases, with the two stone-former sets being very close in value, while the control value is lower.

Thus, the 'reverse engineering' method using the blood and urine concentration values to determine risk points within the nephron can be seen to yield similar results to those generated by the simulation process of Robertson [10].

Conclusion

Computer simulation of physiological processes has been applied to a wide range of medical problems, including insulin therapy in the treatment of diabetes [40, 41] and kidney stone formation [4, 8–10]. Here we show the potential for calculations of a mineral saturation index with clinically useful implications.

Monitoring urolithiasis routinely involves urinalysis. Since the kidney stone formation process has it origin in the nephron, for the purpose of assessing the risk of stone disease, nephron fluid composition is more important than the urine composition itself. However, the measurement of the composition of fluid within nephrons is clinically impractical. The model developed here provides information about the saturation states of substances within the nephron as they relate to given urinalysis results. We consider that the diagnostic value of urinalysis can, therefore, be enhanced in this way.

However, it should be emphasised that factors related to nucleation and crystallisation kinetics of solid phases are not included in this model. In accordance with Ostwald's Rule of Stages, it is *assumed* that brushite, the least stable crystalline Ca phosphate phase, precipitates first. The further development, or inhibition, of stone formation cannot as yet be predicted by the present (or any other) chemical speciation model.

Appendix

A computer program has been developed using the programming language Ada to simulate the ultrafiltration and reabsorption processes in the kidney. A matrix of reabsorption factors has been constructed from published data to quantify what proportion of the original amount of the substances under consideration entering the Bowman's space via ultrafiltration is reabsorbed [8]. Every substance is associated with a sequence of values representing the reabsorption quantity in each of the ten segments of the nephron. The following function is used to work out the change in amount of substance, y, in the fluid in the lumen using the values in the matrix, R:

Journal : Large 240 | Article No : 1172 | Pages : 8 | MS Code : 1172 | Dispatch : 18-11-2019

Table 3 Long nephron concentrations UK N (mmol/L)

Subst	BC	PCT	PR	tDL	tAL	TAL	MD	DT	CT	CCD	MCD	Calyx
Na^+	140.00	141.01	143.88	329.15	329.15	114.70	123.83	121.64	41.02	15.73	91.22	91.22
K^+	4.00	2.01	3.61	8.26	8.26	1.81	2.15	2.67	3.82	7.16	41.52	41.52
Ca^{2+}	1.47	1.64	1.98	4.53	4.53	1.74	1.34	0.76	0.82	0.83	3.29	3.29
Mg^{2+}	0.40	0.65	1.00	2.29	2.29	0.64	0.76	0.94	0.52	0.40	2.30	2.30
C^-	125.00	152.55	85.09	194.66	194.66	142.09	146.42	138.86	28.25	13.96	80.99	80.99
PO_4^{2-}	1.50	0.98	0.54	1.23	1.23	1.23	1.46	1.80	1.94	2.91	16.90	16.90
C_2O_2	0.00	0.00	0.01	0.01	0.01	0.01	0.02	0.02	0.02	0.03	0.20	0.20
SO_4^{2-}	0.40	0.47	0.37	0.85	0.85	0.85	1.01	1.25	1.34	2.02	11.70	11.70
Cit	0.10	0.03	0.05	0.12	0.12	0.12	0.15	0.18	0.19	0.29	1.69	1.69
Creat	0.11	0.20	0.36	0.83	0.83	0.83	0.99	1.22	1.32	1.98	11.46	11.46
Urea	5.46	8.23	13.73	31.40	31.40	29.64	34.87	42.35	41.95	62.52	338.25	338.25
$Uric^-$	0.25	0.26	0.06	0.13	0.13	0.13	0.15	0.19	0.20	0.31	1.77	1.77
NH_3	0.00	0.13	0.48	1.09	1.09	0.40	0.48	0.59	0.64	1.56	12.42	12.42
HCO_3	24.00	22.22	20.79	47.57	47.57	29.26	34.84	43.10	14.47	0.39	2.24	2.24

$$y_s^i = y_{s-1}^i - \frac{R[s,i]}{100} y_0^i \quad 1 \le s \le 10,$$

where y_0^i is the amount of substance i that enters the Bowman's space via ultrafiltration; y_s^i is the amount of substance i at the end of the nephron section under consideration; y_{s-1}^i is the amount of substance i at the end of the previous nephron section; $R[s, i]$ is the percentage of substance i reabsorbed in the nephron section under consideration.

An analogous equation applies to the total volume of the solution which is needed to calculate the concentrations of the substances under consideration.

The calculations given in this paper represent a particular snap shot of current knowledge and it is important to understand that changes will no doubt be made in future to deal with matters such as improved equilibrium constants, changes in the reabsorption factors and other areas where improved information becomes available.

To implement the 'reverse model', adjustments are made to the values in the reabsorption matrix, the value of the adjustment applied is calculated from the ratio of concentration in the urine under consideration and the urine concentrations produced using the standard reabsorption values, to alter the final result for the urine values to the specified value.

Table 4 Long nephron concentrations UK RSF (mmol/L)

Subst	BC	PCT	PR	tDL	tAL	TAL	MD	DT	CT	CCD	MCD	Calyx
Na^+	145.00	146.02	148.96	341.75	341.75	118.97	128.49	126.68	42.66	16.20	111.11	111.11
K^+	4.20	2.10	3.77	8.65	8.65	1.84	2.20	2.73	3.96	7.54	51.71	51.71
Ca^{2+}	1.50	1.69	2.06	4.72	4.72	1.90	1.53	0.98	1.06	1.20	6.33	6.33
Mg^{2+}	0.40	0.65	1.00	2.30	2.30	0.63	0.75	0.93	0.51	0.37	2.55	2.55
Cl^-	125.00	152.47	84.74	194.40	194.40	141.62	145.85	138.55	26.95	11.80	80.94	80.94
PO_4^{2-}	1.50	1.11	0.88	2.01	2.01	2.01	2.39	2.97	3.21	4.87	33.41	33.41
C_2O_2	0.00	0.00	0.01	0.02	0.02	0.02	0.03	0.03	0.04	0.06	0.38	0.38
SO_4^{2-}	0.35	0.45	0.46	1.05	1.05	1.05	1.25	1.56	1.68	2.55	17.47	17.47
Cit	0.30	0.02	0.03	0.08	0.08	0.08	0.10	0.12	0.13	0.19	1.33	1.33
Creat	0.11	0.20	0.36	0.83	0.83	0.83	0.99	1.23	1.33	2.02	13.85	13.85
Urea	5.46	7.76	12.62	28.95	28.95	26.74	31.33	37.94	36.38	54.65	338.05	338.05
$Uric^-$	0.25	0.27	0.07	0.17	0.17	0.17	0.20	0.25	0.27	0.42	2.86	2.86
NH_3	0.00	0.13	0.47	1.07	1.07	0.39	0.47	0.58	0.64	1.56	14.70	14.70
HCO_3	24.00	22.22	20.78	47.68	47.68	29.32	34.93	43.39	14.59	0.33	2.24	2.24

Journal : Large 240 | Article No : 1172 | Pages : 8 | MS Code : 1172 | Dispatch : 18-11-2019

Table 5 Long nephron concentrations KSA RSF (mmol/L)

Subst	BC	PCT	PR	tDL	tAL	TAL	MD	DT	CT	CCD	MCD	Calyx
Na^+	145.00	146.01	148.92	341.95	341.95	118.96	128.49	126.80	42.60	16.01	116.31	116.31
K^+	4.20	2.07	3.73	8.56	8.56	1.71	2.04	2.54	3.77	7.29	52.94	52.94
Ca^{2+}	1.50	1.67	2.01	4.62	4.62	1.76	1.35	0.74	0.80	0.80	3.80	3.80
Mg^{2+}	0.40	0.65	1.00	2.30	2.30	0.63	0.75	0.93	0.51	0.38	2.74	2.74
Cl^-	125.00	152.44	84.63	194.32	194.32	141.48	145.68	138.45	26.55	11.14	80.92	80.92
PO_4^{2-}	1.50	1.13	0.91	2.09	2.09	2.09	2.49	3.09	3.34	5.09	36.97	36.97
C_2O_2	0.00	0.00	0.01	0.03	0.03	0.03	0.04	0.05	0.06	0.08	0.61	0.61
SO_4^{2-}	0.35	0.46	0.49	1.14	1.14	1.14	1.35	1.68	1.82	2.77	20.13	20.13
Cit	0.30	0.01	0.02	0.04	0.04	0.04	0.05	0.06	0.07	0.10	0.75	0.75
Creat	0.11	0.20	0.36	0.83	0.83	0.83	0.99	1.24	1.34	2.03	14.78	14.78
Urea	5.46	7.62	12.29	28.21	28.21	25.87	30.27	36.60	34.69	52.22	337.97	337.97
$Uric^-$	0.25	0.27	0.10	0.22	0.22	0.22	0.26	0.33	0.36	0.54	3.93	3.93
NH_3	0.00	0.34	1.23	2.84	2.84	1.04	1.24	1.54	1.68	4.16	41.58	41.58
HCO_3	24.00	22.22	20.78	47.72	47.72	29.34	34.96	43.48	14.62	0.31	2.24	2.24

Tables 3, 4 and 5 show the total concentrations of the substances under consideration along the length of the nephron for the three sets of subjects used in this paper.

A copy of the computer program may be requested by contacting the corresponding author.

References

1. Grases F, Costa-Bauzá A, Garcia-Ferragut L (1998) Biopathological crystallization: a general view about the mechanisms of renal stone formation. Adv Colloid Interface Sci 74:169–194
2. Kallidonis P, Liourdi D, Liatsikos E (2011) Medical treatment for renal colic and stone expulsion. Eur Urol Suppl 10:415–422
3. Tiselius HG (2011) Who forms stones and why? Eur Urol Suppl 10:408–414
4. Hill MG, Königsberger E, May PM (2017) Mineral precipitation and dissolution in the kidney. Am Mineral 102:701–710
5. Tiselius HG (1982) An improved method for the routine biochemical evaluation of patients with recurrent calcium oxalate stone disease. Clin Chim Acta 122:409–418
6. Milosevic D, Batinic D, Konjevoda NBP, Stambuk N, Votava-Raic A, Fumic VBK, Rumenjak V, Stavljenic-Rukavina A, Nizic L, Vrljicak K (1998) Determination of urine supersaturation with computer program Equil 2 as a method for estimation of the risk of urolithiasis. J Chem Inf Comput Sci 38:646–650
7. Laube N, Schneider A, Hesse A (2000) A new approach to calculate the risk of calcium oxalate crystallization from unprepared native urine. Urol Res 28:274–280
8. Hill MG (2019) A chemical model to investigate the risk of kidney stone formation in humans in terms of urinary supersaturation. PhD thesis, Murdoch University
9. Rodgers AL, Allie-Hamdulay S, Jackson G, Tiselius HG (2011) Simulating calcium salt precipitation in the nephron using chemical speciation. Urol Res 39:245–251
10. Robertson WG (2015) Potential role of fluctuations in the composition of renal tubular fluid through the nephron in the initiation of Randall's plugs and calcium oxalate crystalluria in a computer model of renal function. Urolithiasis 43(Supplement 1):S93–S107
11. Tiselius H, Lindbäck B, Fornander AM, Nilsson MA (2009) Studies on the role of calcium phosphate in the process of calcium oxalate crystal formation. Urol Res 37:181–192
12. Højgaard I, Tiselius HG (1999) Crystallization in the nephron. Urol Res 27:397–403
13. Tiselius HG (1997) Estimated levels of supersaturation with calcium phosphate and calcium oxalate in the distal tubule. Urol Res 25:153–159
14. Kok DJ (1997) Intratubular crystallization events. World J Urol 15:219–228
15. Söhnel O, Grases F (1995) Calcium oxalate monohydrate renal calculi. Formation and development mechanism. Adv Colloid Interface Sci 59:1–17
16. Grases F, Costa-Bauzá A, Gomila I, Ramis M, García-Raja A, Prieto RM (2012) Urinary pH and renal lithiasis. Urol Res 40:41–46
17. Robertson WG, Scurr DS, Bridge CM (1981) Factors influencing the crystallisation of calcium oxalate in urine–critique. J Cryst Growth 53:182–194
18. Tiselius HG (2011) A hypothesis of calcium stone formation: an interpretation of stone research during the past decades. Urol Res 39:231–243
19. Rodgers A, Webber D, Hibberd B (2015) Experimental determination of multiple thermodynamic and kinetic factors for nephrolithiasis in the urine of healthy controls and calcium oxalate stone formers: does a universal discriminator exist? Urolithiasis 43:479–487
20. Coe FL, Evan A, Worcester E (2011) Pathophysiology-based treatment of idiopathic calcium kidney stones. Clin J Am Soc Nephrol 6:2083–2092
21. Baumann JN, Affolter B (2014) From crystaluria to kidney stones, some physicochemical aspects of calcium nephrolithiasis. World J Nephrol 3:256–267
22. Söhnel O, Grases F (2011) Supersaturation of body fluids, plasma and urine, with respect to biological hydroxyapatite. Urol Res 39:429–436
23. Asplin JR, Mandel NS, Coe FL (1996) Evidence for calcium phosphate supersaturation in the loop of Henle. Am J Physiol 270:F604–F613
24. Luptak J, Bek-Jensen H, Fornander AM, Højgaard I, Nilsson MA, Tiselius H (1994) Crystallization of calcium oxalate and calcium phosphate at superstauration levels corresponding to those in different parts of the nephron. Scan Microsc 8:47–62

Journal : Large 240 | Article No : 1172 | Pages : 8 | MS Code : 1172 | Dispatch : 18-11-2019

25. Grases F, Villacampa AI, Söhnel O, Königsberger E, May PM (1997) Phosphate composition of precipitates from urine-like liquors. Cryst Res Technol 32:707–715
26. Johnsson MSA, Nancollas GH (1992) The role of brushite and octacalcium phosphate in apatite formation. Crit Rev Oral Biol Med 3:61–82
27. Pak CYC (1969) Physicochemical basis for formation of renal stones of calcium phosphate origin: calculation of the degree of saturation of urine with respect to brushite. J Clin Investig 48:1914–1922
28. Pak CYC (1981) Potential etiologic role of brushite in the formation of calcium (renal) stones. J Cryst Growth 53:202–208
29. Pak CYC, Rodgers K, Poindexter JR, Sakhaee K (2008) New methods of assessing crystal growth and saturation of brushite in whole urine: effect of pH, calcium and citrate. J Urol 180:1532–1537
30. Coe FL, Parks JH, Nakagawa Y (1992) Inhibitors and promoters of calcium oxalate crystallization. their relationship to the pathogenesis and treatment of nephrolithiasis. In: Coe FL, Favus MJ (eds) Disorders of bone and mineral metabolism, vol 35. Raven Press Ltd, New York, pp 757–799
31. Rabadjieva D, Tepavitcharova S, Sezanova K, Gergulova R (2016) Chemical equilibria modeling of calcium phosphate precipitation and transformation in simulated physiological solutions. J Solut Chem 45:1620–1633
32. Sawada K (1997) The mechanisms of crystallization and transformation of calcium carbonates. Pure Appl Chem 69:921–928
33. Zhang J, Wang L, Putnis C (2019) Underlying role of brushite in pathological mineralization of hydroxyapatite. J Phys Chem B 123:2874–2881
34. Atherton JC (2006) Function of the nephron and the formation of urine. Anaesth Intensive Care Med 7:221–226
35. Good DW, Knepper MA (1985) Ammonia transport in the mammalian kidney. Am J Physiol 248:F459–F471
36. May PM, Murray K (1991) JESS, a joint expert speciation system—I. Raison d'être. Talanta 38:1409–1417
37. May PM, Murray K (1991) JESS, a joint expert speciation system—II. The thermodynamic database. Talanta 38:1419–1426
38. May PM (2015) JESS at thirty: strengths, weaknesses and future needs in the modelling of chemical speciation, Appl Geochem 55:3–16
39. May PM, Rowland D (2018) JESS, a joint expert speciation system—VI: thermodynamically-consistent standard Gibbs energies of reaction for aqueous solutions. N J Chem 42:7617–7629
40. Cavan D, Hovorka R, Hejlesen O, Andreassen S, Sonksen P (1996) Use of the DIAS model to predict unrecognised hypoglycaemia in patients with insulin dependent diabetes. Comput Methods Prog Biomed 50:241–246
41. Hill M (2010) A personal experience of using computer technology to assist with the treatment of diabetes. In: Proceedings of the UKACC international conference on control, Coventry, UK, pp 417–422. https://doi.org/10.1049/ic.2010.0319

Journal : Large 240 | Article No : 1172 | Pages : 8 | MS Code : 1172 | Dispatch : 18-11-2019